JOTCS A
Journal of the Turkish Chemical Society
Section: A
Chemistry
TURKISH CHEMICAL SOCIETY

Half-metallic Ferromagnetism in Fe-doped and Zn-vacancy Defected ZnSe: First-Principles Investigation

Vusala N. Jafarova[1,2*] ORCID, Aynur N. Jafarova[1] ORCID, Asmer A. Abdullayeva[1], Musaver A. Musaev[1] ORCID

[1]Azerbaijan State Oil and Industry University, 20 Azadlig Ave., AZ-1010, Baku, Azerbaijan.
[2]Khazar University, 41 Mehseti Str., AZ1096, Baku, Azerbaijan.

Abstract: The magnetic properties of defected ZnSe wurtzite systems were theoretically investigated using Density Functional Theory and Local Spin Density Approximation. From this first principal study, it was determined that pure ZnSe is a non-magnetic direct band gap semiconductor. Investigations show that adding the iron and the presence of a single Zn vacancy defect leads to the magnetization of ZnSe. The results of total energy calculations show that a ferromagnetic state is favorable when Zn is replaced with Fe. The ferromagnetic alignment in Fe-doped ZnSe wurtzite compound behaves in high-spin and half-metallic states.

Keywords: ZnSe: Fe, Magnetic properties, Ferromagnetism, Half-metallic.

Submitted: January 25, 2024. **Accepted:** July 12, 2024.

Cite this: Jafarova VN, Jafarova AN, Abdulleyeva AA, Musaev MA. Half-metallic Ferromagnetism in Fe-doped and Zn-vacancy Defected ZnSe: First-Principles Investigation. JOTCSA. 2024;11(3): 1297-302.

DOI: https://doi.org/10.18596/jotcsa.1425866

***Corresponding author's E-mail:** vcafarova@beu.edu.az

1. INTRODUCTION

Diluted magnetic semiconductors (DMSs) attract research interest for the semiconducting and magnetic properties in the same compound (1-4). 3d transition-metal (TM=V, Cr, Mn, Fe, Co, Ni) doped II-VI Zn-based semiconductor compounds have revealed their potential for technical application according to their wide band gap of 2.70 eV (5). ZnSe is ideally appropriate for the fabrication of photodetectors, CO_2 laser focusing lenses, sensors, solar cells, and other photovoltaic applications (5,6). This material can be applied for the production of optoelectronic devices such as light emitters and detectors (7-9).

DMSs based on II-VI group compounds have been attracting great interest as promising materials for new spin electronic devices because these compounds show ferromagnetism, whose Curie temperature depends on the carrier concentration (10,11). For industrial applications of DMSs, room-temperature ferromagnetism is strongly required.

The DMSs' first-principles studies have allowed the production of new types of materials with possible technological applications in Engineering, Medicine, and Environmental Chemistry.

In Refs. (12,13) reported that Fe-doped and as-grown ZnSe solid solutions show a paramagnetic nature at low temperatures. In theoretical work (14), the authors predicted lower FM properties and the presence of a spin-glass state for ZnSe: Fe solid solutions. In (15), reported results are in contradiction with the prediction of antiferromagnetic (AFM), paramagnetic, and spin-glass (SG) magnetic states in Zn(Fe)Se zinc-blende crystal. D.P. Rai and co-workers studied (16) 5 Zn vacancies in the monolayer hexagonal ZnSe 18-atom supercell modeled by 3×3×1 transferred based on the DFT. They reported that the Zn vacancy makes the FM state of ZnSe. Nevertheless, there is no common opinion about the mechanism of magnetism in iron-doped ZnSe, and the views of different researchers are opposite.

This work is based on the DFT-LSDA+U; a detailed theoretical study of magnetic properties for Fe^{2+} doped ZnSe structure is provided. In our previous work (17), we obtained that the calculated energy band gap (2.7 eV) of ZnSe is closer to the known experimental results. The results of magnetic properties of $Zn_{1-x}Fe_xSe$ (x=1/8, 1/16) systems also provide useful information for future research studies to understand the origin of ferromagnetism

in these systems. However, a lower energy state in the FM state compared to the AFM state indicates a stable magnetic state.

2. THEORETICAL SECTION

2.1. Investigation Method

The calculations were carried out for the Zn(Fe)Se systems with 32 and 96 atoms by the DFT method (18) within Local Spin Density Approximation (LSDA) (19) implemented Atomistix ToolKit code within incorporated Mulliken population analysis. The interactions between the electrons and ions, as well as exchange correlation, were described by the Fritz-Haber-Institute ion pseudopotentials (20). The Kohn-Sham wave functions (21) are solved in a linear combination of atomic orbitals (LCAO), and the cutoff of kinetic energy for electrons is 150 Ry. The supercells containing dopant atoms and vacancies were geometry optimized, and the force and stress tolerances are about less than 0.01 eV/Å and 0.01 eV/Å^3, respectively. The reciprocal space integration was performed with a 5×5×5 Monkhorst-Pack grid (22). To simulate the antiferromagnetic states of DMS systems, cations (Zn) were replaced randomly by $Fe^{\uparrow}_{x/2}$ (for spin-up) and $Fe^{\downarrow}_{x/2}$ (for spin-down) ions.

3. RESULTS AND DISCUSSION

3.1. Magnetic Properties of Fe-doped ZnSe

Using the DFT-LSDA method within Hubbard U correction, the magnetic properties from Mulliken Population analysis were studied using Atomistic ToolKit software. In work (23), the authors summarized the results of magnetic properties of TM-doped ZnSe nanosheet using the DFT-GGA method. They reported that the magnetic moment for Fe atom doped nanosheet is about 4.89 μ_B. In the present case, the model used for TM^{2+} doped ZnSe is a 5×5×5 MP grid for 32 and 96-atom supercells with one or two Zn atoms substituted by TM dopant atoms. In order to calculate magnetic properties, iron atoms have been modeled to replace the site of Zn atoms, as shown in Figure 1. In all figures of spin-polarization structures, the magnetic moments of atoms are described by green arrows.

For recent simulations, the FM and AFM states of Fe-doped ZnSe supercells can be described as $Zn_{1-x}Fe^{\uparrow}_{x}Se$ and $Zn_{1-x}Fe^{\uparrow}_{x/2}Fe^{\downarrow}_{x/2}Se$, correspondingly. Moreover, in order to check the stability of these phases, the differences in energy between both states ($\Delta E=E_{AFM}$ - E_{FM}) of these systems have been calculated. The obtained values are given in Table 1.

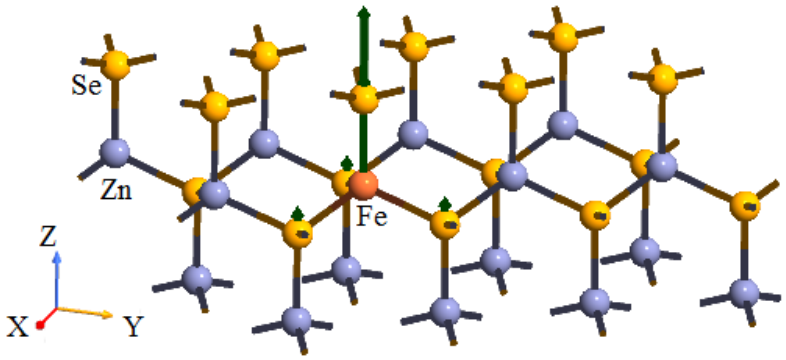

Figure 1: The spin-polarization for $Zn_{15}Fe_1Se_{16}$ supercell (Zn-gray, Se-yellow, Fe-brown).

Table 1: The DFT-LSDA+U results for different $Zn_{1-x}Fe_xSe$ supercells.

Supercell	x	μ(Fe), μ_B per Fe	$(E_{AFM}-E_{FM})/2$, *meV* per Fe
$Zn_{15}Fe_1Se_{16}$	0.0625	4.004	-
$Zn_{14}Fe_2Se_{16}$	0.125	4.0	0.205
$Zn_{47}Fe_1Se_{48}$	0.0208(3)	4.0	-
$Zn_{46}Fe_2Se_{48}$	0.04166	3.9975	0.035

The first-principles results of the total energy differences ΔE show that the antiferromagnetic (AFM) state is more stable than the ferromagnetic (FM) spin ordering one when Fe^{2+} substitutes on Zn sites. Similar behavior is reported for TM co-doping ZnSe cubic structures in Ref. (24).

Current studies show that a single Fe(Zn) substitution leads to magnetization, and the magnetic moment for 96-atom systems is around 4 μ_B, which is consistent with the band structure results. This value corresponds to the GGA obtained result (4.89 μ_B) for Fe-doped ZnSe nanosheet (23). In the case of Fe(Zn), Zn atoms have a less weakening effect on the magnetic field (~ -0.05 μ_B), the magnetization created mainly by the impurity atom (~ 3.5 μ_B from Fe atom including 3.359 μ_B from *d*-electrons). The positive magnetic moments of all Se atoms (~ 0.6 μ_B) are small in magnitude.

3.2. ZnSe:Fe with Zn Vacancy-defect

In this section, we investigated two cases of Zn vacancy-defect positions in ZnSe systems. The presence of *Zn* vacancy and Fe-doped ZnSe systems (Figure 2) lead to significant changes. The Se atoms, which are located neighboring the vacancy position

and chemically bonded to the iron, create a positive magnetic moment and make up for the negative moment of the zinc atoms.

For Fe(Zn) replacement and availability of one Zn vacancy positioned far from the impurity atom, the computed total moment of the 96-atom supercell is 5.594 μ_B, with main partial magnetic moments from Fe (3.607 μ_B) and 48 Se atoms (2.774 μ_B). The significant contributions relate to the 4 Se atoms nearby and chemical bonding with impurity atom (0.704 μ_B) and 4 Se with dangling bonds from nearly the vacancy position (1.265 μ_B). 46 Zn atoms weaken the total magnetic moment of the system (-0.787 μ_B). Thus, the total magnetization of the supercell increases by the amount of ~1.6 μ_B due to the defect.

In the second case, the vacancy site is chosen in such a way that one of the host selenium atoms bonded with an impurity atom loses one chemical bond due to the vacancy. We obtain the strength of the magnetization by 0.353 μ_B. The impurity iron atom makes great moment (3.605 μ_B), and 46 Zn atoms weaken total magnetization by the quantity -0.37 μ_B. The basic contributions from 48 Se atoms: 2.712 μ_B (4 Se atoms bonding with impurity atom (0.525 μ_B), 4 Se atoms losing the chemical bond due to vacancy (1.275 μ_B)). In comparison with the vacancy-free case, total magnetic field strengthening is ~1.95 μ_B.

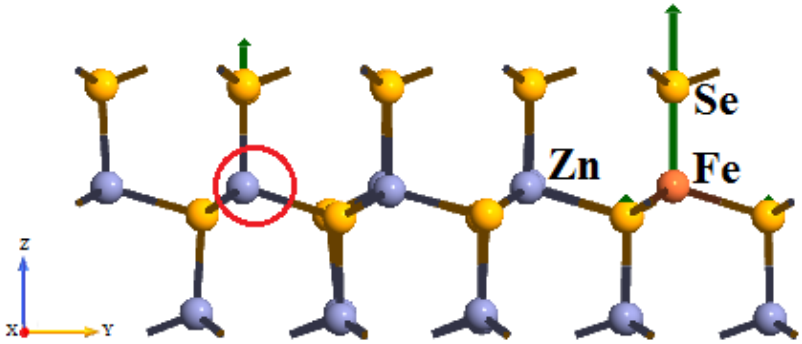

Figure 2: The spin polarization structure for $Zn_{14}Fe_1Se_{16}$ with one Zn vacancy.

The first-principles results for the wide band gaps of 32-atom ZnSe supercells are 2.60/2.60 eV and 1.22/1.39 eV for up and down states, correspondingly. The total magnetic moment for the $Zn_{14}Fe_1Se_{16}$ system is ~5.9 μ_B.

Figures 3 and 4 show the calculated spin-polarized band structures and total density of states for the Fe-doped and Zn-vacancy-defected $Zn_{46}Fe_1Se_{48}$ 96-atom supercell.

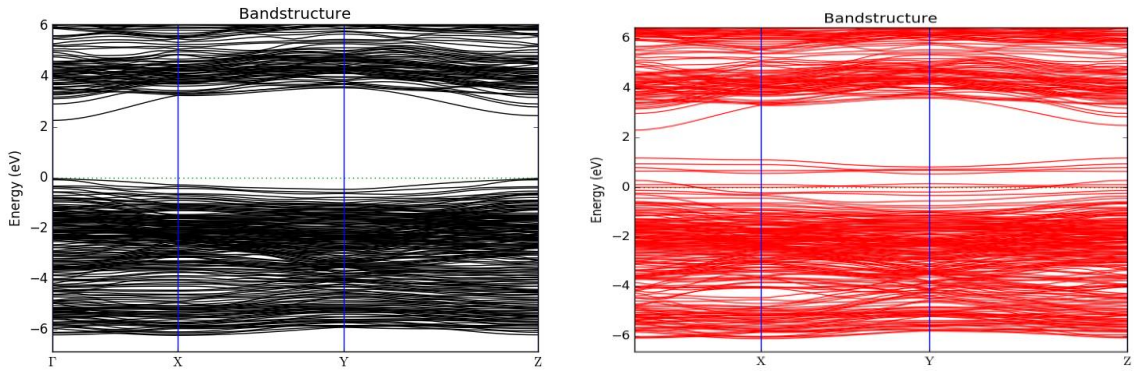

Figure 3: The obtained band structures for Fe-doped and Zn-vacancy defected $Zn_{46}Fe_1Se_{48}$ for spin-up (black color) and spin-down states (red color).

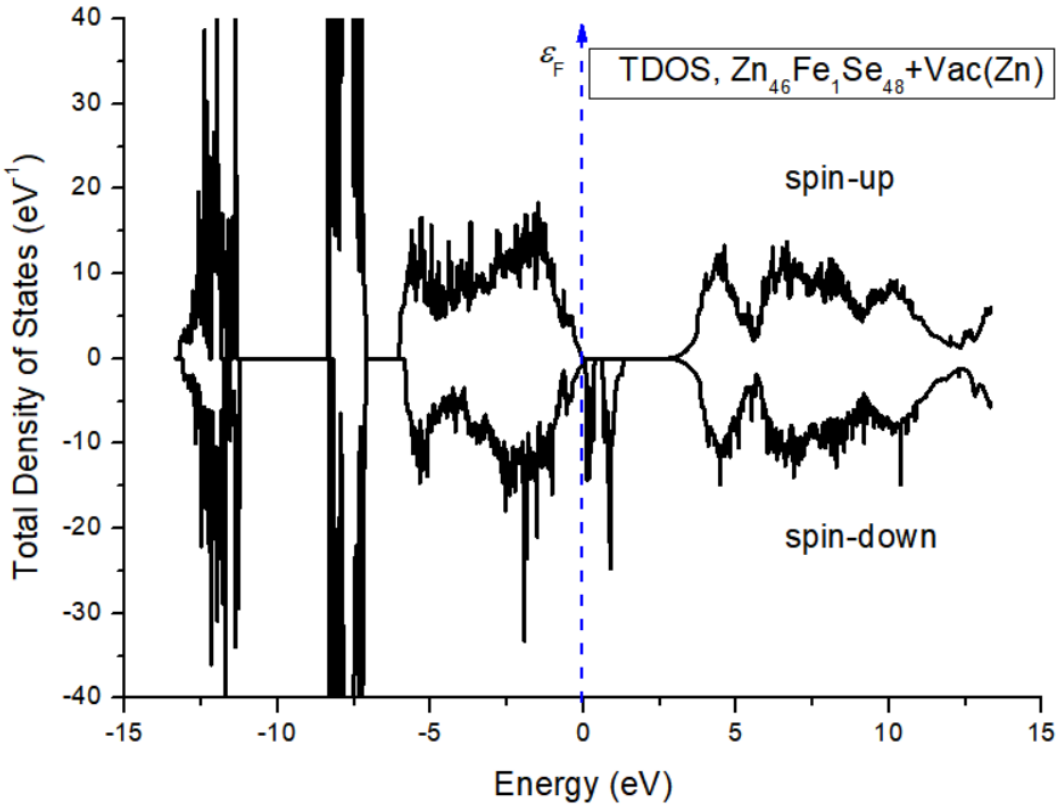

Figure 4: The DFT-LSDA+U calculated TDOS of $Zn_{46}Fe_1Se_{48}$ system with Zn vacancy.

DFT-LSDA+U calculations revealed that Fe(Zn) replacement and the availability of one Zn defect in the ZnSe supercell is the most effective for strengthening the magnetization. Thus, the shift of moment of the system due to one Zn vacancy side is (1.6 ÷ 1.9) μ_B, depending on the chosen location of the defect.

4. CONCLUSION

In summary, the magnetic properties of iron-doped ZnSe systems are studied by DFT using the LSDA+U method. The investigations performed for 32- and 96-atom Fe-doped ZnSe supercells show that Zn substitutions by Fe lead to a ferromagnetic spin ordering. The FM alignment in the Zn(Fe)Se systems behaves as semi-metallic ferromagnetism manifests itself in a significant density of impurity states. The band gap energy of ZnSe supercells is observed to increase after the Fe atom replaces Zn and leads to the magnetization of systems. The results of total energy calculations of ZnSe almost present a stable antiferromagnetic state when Fe^{2+} ions are substituted on Zn sites.

In this work, we hope to contribute significantly to the investigation of DMSs and their possible technological applications for society's benefit.

5. CONFLICT OF INTEREST

The authors declare that they have no known competing financial interests or personal relationships that could have appeared to influence the work reported in this paper.

7. REFERENCES

1. Munekata H, Ohno H, von Molnar S, Segmüller A, Chang LL, Esaki L. Diluted magnetic III-V semiconductors. Phys Rev Lett [Internet]. 1989 Oct 23;63(17):1849–52. Available from: <URL>.

2. Ohno H, Shen A, Matsukura F, Oiwa A, Endo A, Katsumoto S, et al. (Ga,Mn)As: A new diluted magnetic semiconductor based on GaAs. Appl Phys Lett [Internet]. 1996 Jul 15;69(3):363–5. Available from: <URL>.

3. Dietl T. A ten-year perspective on dilute magnetic semiconductors and oxides. Nat Mater [Internet]. 2010 Dec 23;9(12):965–74. Available from: <URL>.

4. Dietl T, Ohno H. Dilute ferromagnetic semiconductors: Physics and spintronic structures. Rev Mod Phys [Internet]. 2014 Mar 24;86(1):187–251. Available from: <URL>.

5. Neumark GF, Park RM, Depuydt JM. Blue-green diode lasers. Phys Today [Internet]. 1994 Jun 1;47(6):26–32. Available from: <URL>.

6. Karzel H, Potzel W, Köfferlein M, Schiessl W, Steiner M, Hiller U, et al. Lattice dynamics and hyperfine interactions in ZnO and ZnSe at high external pressures. Phys Rev B [Internet]. 1996 May 1;53(17):11425–38. Available from: <URL>.

7. Adetunji BI, Adebambo PO, Adebayo GA. First principles studies of band structure and electronic properties of ZnSe. J Alloys Compd [Internet]. 2012 Feb;513:294–9. Available from: <URL>.

8. Haase MA, Qiu J, DePuydt JM, Cheng H. Blue-green laser diodes. Appl Phys Lett [Internet]. 1991 Sep 9;59(11):1272–4. Available from: <URL>.

9. Eason DB, Yu Z, Hughes WC, Roland WH, Boney C, Cook JW, et al. High-brightness blue and green light-emitting diodes. Appl Phys Lett [Internet]. 1995 Jan 9;66(2):115–7. Available from: <URL>.

10. A. Medvedkin G, Takayuki Ishibashi TI, Takao Nishi TN, Koji Hayata KH, Yoichi Hasegawa YH, Katsuaki Sato KS. Room temperature ferromagnetism in novel diluted magnetic semiconductor $Cd_{1-x}Mn_xGeP_2$. Jpn J Appl Phys [Internet]. 2000 Oct 1;39(10A):L949. Available from: <URL>.

11. Ohno H. Properties of ferromagnetic III–V semiconductors. J Magn Magn Mater [Internet]. 1999 Oct;200(1–3):110–29. Available from: <URL>.

12. Mayer AM. Lecture notes in physics. 1982;152:109–19. Available from: <URL>.

13. Furdyna JK. Diluted magnetic semiconductors. J Appl Phys [Internet]. 1988 Aug 15;64(4):R29–64. Available from: <URL>.

14. Katayama-Yoshida H, Sato K. Spin and charge control method of ternary II–VI and III–V magnetic semiconductors for spintronics: theory vs. experiment. J Phys Chem Solids [Internet]. 2003 Sep;64(9–10):1447–52. Available from: <URL>.

15. Khan MS, Shi L, Zou B. Impact of vacancy defects on optoelectronic and magnetic properties of Mn-doped ZnSe. Comput Mater Sci [Internet]. 2020 Mar;174:109493. Available from: <URL>.

16. Rai DP, Laref A, Khuili M, Al-Qaisi S, Vu T V., Vo DD. Electronic, magnetic and optical properties of monolayer (ML) hexagonal ZnSe on vacancy defects at Zn sites from DFT-1/2 approach. Vacuum [Internet]. 2020 Dec;182:109597. Available from: <URL>.

17. Jafarova V., Musaev M. First-principles study of structural and electronic properties of ZnSe with wurtzite structure. Tech Rom J Appl Sci Technol [Internet]. 2023 Feb 9;6:42–6. Available from: <URL>.

18. Hohenberg P, Kohn W. Inhomogeneous electron gas. Phys Rev [Internet]. 1964 Nov 9;136(3B):B864–71. Available from: <URL>.

19. Parr RG, Yang W. Density-functional theory of atoms and molecules [Internet]. New York: Oxford University Press; 1989. Available from: <URL>.

20. Fuchs M, Scheffler M. Ab initio pseudopotentials for electronic structure calculations of poly-atomic systems using density-functional theory. Comput Phys Commun [Internet]. 1999 Jun;119(1):67–98. Available from: <URL>.

21. Lundqvist S, March NH. Theory of the Inhomogeneous Electron Gas [Internet]. Lundqvist S, March NH, editors. Boston, MA: Springer US; 1983. 425 p. Available from: <URL>.

22. Monkhorst HJ, Pack JD. Special points for Brillouin-zone integrations. Phys Rev B [Internet]. 1976 Jun 15;13(12):5188–92. Available from: <URL>.

23. Chen XL, Huang BJ, Feng Y, Wang PJ, Zhang CW, Li P. Electronic structures and optical properties of TM (Cr, Mn, Fe or Co) atom doped ZnSe nanosheets. RSC Adv [Internet]. 2015;5(128):106227–33. Available from: <URL>.

24. Behloul M, Salmani E, Ez-Zahraouy H, Benyoussef A. Theoretical investigation of electronic, magnetic and optical properties of ZnSe doped TM and co-doped with MnTM (TM: Fe, Cr, Co): AB-initio study. J Magn Magn Mater [Internet]. 2016 Dec;419:233–9. Available from: <URL>.